River water temperature quantiles as thermal stress indicators: Case study in Switzerland

Zina Souaissi [*], Taha B.M.J. Ouarda, André St-Hilaire

Canada Research Chair in Statistical Hydro-Climatology, Institut national de la recherche scientifique, Centre Eau Terre Environnement, INRS-ETE, 490 De la Couronne, Québec City, QC, Canada

ARTICLE INFO

ABSTRACT

The variability of the river water thermal regime has important consequences on the environment and aquatic habitat. In 25 independent and identically distributed stations in Switzerland, local frequency analysis is used to quantify extreme river temperatures. Probability distributions are fitted to the data to estimate maximum water temperatures corresponding to different return periods. The goodness of fit of statistical distributions are evaluated using the Akaike and Bayesian Information Criteria. L-moment ratio diagrams are also used to validate the choices of appropriate candidate distributions. Results show that for high altitude stations the two-parameter Weibull (W2) distribution is the most adequate distribution to represent extreme river water temperatures while for low altitude stations the most commonly selected distributions are the Normal (N) and Inverse Gamma (IG). The L-moment ratio diagrams confirm the results of the local frequency analysis. These results point to the presence of a regional homogeneity in the thermal regime of the study area. River temperature quantiles are compared to know thresholds above which thermal stress occurs for a relatively ubiquitous salmonid species in Europe (Brown trout).

1. Introduction

Stream temperature is one of the most important variables in the study of aquatic habitats (Caissie, 2006). It has a great influence on water quality (Hosseini et al., 2017; Mujere and Moyce, 2018), concentration of chemicals (Ficklin et al., 2013; Petts, 2000), and ecosystem health. In addition, it affects the life cycle of many fish, including salmonids (Brandão et al., 2018; Jonsson and Jonsson, 2009). Climate change will impact seasonal and daily variations of water temperature (Isaak et al., 2012; Isaak and Rieman, 2013; Kwak et al., 2017; Niedrist et al., 2018). Deforestation, flow control, and dam construction can also have significant impacts on river temperatures (Caissie, 2006; Dan Moore et al., 2005; Maheu et al., 2016). The variability in river thermal regime has garnered increasing interest over the last decades from the hydrologic community (Ashley Steel et al., 2016; Ouellet et al., 2020).

Many authors have focused on understanding the impacts of water temperature on fish growth, mortality, and on aquatic habitats in general (Dugdale et al., 2013; Elliott and Elliott, 2010; Sun and Chen, 2014). Many other research studies have focused on the development of statistical models to predict stream temperature (Beaupré et al., 2020; Benyahya et al., 2007; Boudreault et al., 2019; Dugdale et al., 2017; St-Hilaire et al., 2012; Zhu et al., 2019).

Ectotherms can survive only within a specific temperature range. In Switzerland, several studies have been carried out to identify the threshold of water temperature that generates stress or mortality of brown trout (*Salmo trutta*). For instance, Körner et al. (2008) have shown that water temperature above 19 °C can influence the concentration of vitellogenin (Vtg) in the plasma of brown trout. Wahli et al. (2008) demonstrated the relationship between fish infected by Tetracapsuloides bryosalmonae in Switzerland (where the present study was

Table 1
Probability distribution functions used in the study.

Name	Probability density function	Domain	No. of parameters
Exponential	$f(x) = \frac{1}{(x-m)\propto\sqrt{2\pi}}exp\left\{-\frac{[ln(x-m)-\mu]^2}{2\propto^2}\right\}$	$x > m$	2
Gamma	$f(x) = \frac{\alpha^\lambda}{\Gamma(\lambda)}x^{\lambda-1}e^{-\alpha x}$	$x > 0$	2
Generalized Gamma	$f(x) = \frac{\|s\|\alpha^{s\lambda}}{\Gamma(\lambda)}x^{s\lambda-1}e^{-(\alpha x)^s}$	$x > 0$	3
GEV	$f(x) = \frac{1}{\alpha}\left[1-\frac{k}{\alpha}(x-v)\right]^{\frac{1}{k}-1}exp\left\{-\left[1-\frac{k}{\alpha}(x-v)\right]^{\frac{1}{k}}\right\}$	$x > v + \frac{\alpha}{k} if k < 0 \quad x < v + \frac{\alpha}{k} if k > 0$	3
Gumbel	$f(x) = \frac{1}{\alpha}exp\left[-\frac{x-v}{\alpha}-exp\left(\frac{x-v}{\alpha}\right)\right]$	$-\infty < x \, x < +\infty$	2
Halphen A	$f(x) = \frac{1}{2m^v k_v(2\alpha)}x^{v-1}exp\left[-\alpha\left(\frac{x}{m}+\frac{m}{x}\right)\right]$	$x > 0$	3
Halphen B	$f(x) = \frac{2}{m^{2v}ef_v(\alpha)}x^{2v-1}exp\left[-\left(\frac{x}{m}\right)^2+\alpha\left(\frac{x}{m}\right)\right]$	$x > 0$	3
Inverse Halphen B	$f(x) = \frac{2m^{2v}}{ef_v(\alpha)}x^{-2v-1}exp\left[-\left(\frac{m}{x}\right)^2+\alpha\left(\frac{m}{x}\right)\right]$	$x > 0$	3
Lognormal two parameters	$f(x) = \frac{1}{x\sigma\sqrt{2\pi}}exp\left\{-\frac{(lnx-\mu)^2}{2\sigma^2}\right\}$	$x > 0$	2
Lognormal three parameters	$f(x) = \frac{1}{(x-m)\sigma\sqrt{2\pi}}exp\left\{-\frac{(ln(x-m)-\mu)^2}{2\sigma^2}\right\}$	$x > m$	3
Log-Person type 3	$f(x) = \frac{\alpha^\lambda}{x\Gamma(\lambda)}(lnx-m)^{\lambda-1}e^{-\alpha(lnx-m)}$	$x > e^m$	3
Normal	$f(x) = \frac{1}{\sigma\sqrt{2\pi}}exp\left\{-\frac{(x-\mu)^2}{2\sigma^2}\right\}$	$-\infty < x \, x < +\infty$	2
Person type 3	$f(x) = \frac{\alpha^\lambda}{\Gamma(\lambda)}(x-m)^{\lambda-1}e^{-\alpha(x-m)}$	$x > m$	3
Weibull	$f(x) = \frac{c}{\alpha}\left(\frac{x}{\alpha}\right)^{c-1}exp\left[-\left(\frac{x}{\alpha}\right)^c\right]$	$x > 0$	2
Generalised Pareto	$f(x) = \frac{1}{\alpha}\left(1-\frac{k}{\alpha}x\right)^{\frac{1}{k}-1} if k \neq 0 \quad f(x) = \frac{1}{\alpha}e^{-x/\propto} if k = 0$	$k \leq 0 \quad 0 \leq x < +\infty \quad k > 0 \quad 0 \leq x \leq \propto/k$	2

μ: location parameter.
m: second location parameter (LN3).
α: scale parameter.
k: shape parameter.
s: second shape parameter (GG).
Γ (): gamma function.

conducted) and altitude (the lower the altitude, the higher the temperature, the more infected the fish). According to Elliott (2001), the optimum growth rate of brown trout occurs at 13.1–13.9 °C, and growth ceases below 2.9–3.6 °C and above 18.7–19.5 °C. Several studies have also indicated that when temperature exceeds 15 °C proliferative kidney disease (PKD) becomes more prevalent in brown trout populations (Chilmonczyk et al., 2002; Strepparava et al., 2018). In addition, many studies have also investigated the definition of lethal temperatures. For instance, Elliott (1981) determined the ultimate brown trout lethal temperature (survival for ten minutes) to be 29.7 ± 0.36 °C. Further, Wehrly et al. (2007) focused on the definition of thermal tolerance limits. The upper limit of tolerance over 7 days, for example, was 23.3 °C for the maximum daily mean temperature and 25.4 °C for the maximum daily temperature. These thresholds can be used as thermal indicators in river ecosystems. The present study allows to characterize them in a probabilistic context using frequency analysis. In this initial study, we demonstrate how maximum daily temperature quantiles can be used as an indicator of stress. Temperature quantiles corresponding to low return periods (e.g. one or two years) occur relatively often, whereas those with higher return periods (e.g. 10 or 50 years) are more extreme and occur less often, on average.

Many studies related to river temperature were conducted in Switzerland. They include the development of a hybrid statistical-physically based model to estimate the monthly mean stream temperature of ungauged rivers (Gallice et al., 2015). More recently, Michel et al. (2020) investigated the evolution of river temperature over the last 50 years in 52 Swiss catchments.

To estimate extreme thermal events and their associated return periods, local frequency analysis (LFA) of the water temperature in Swiss rivers was carried out. Quantile estimation depends strongly on the shape of the selected frequency distribution. The choice of the most appropriate distribution of annual maxima or peaks over a selected threshold has received considerable attention for other hydro-climatic variables. For example, Thiombiano et al. (2017) showed that the Generalized Pareto Distribution (GPD) is the most adequate to represent peaks over thresholds of precipitation series in Southeaster Canada. Ouarda et al. (2016) have indicated that the Weibull (W2) is the most widely used distribution in studies related to wind speed data analysis in the United Arab Emirates. Tramblay et al. (2008) indicated that the Log-Normal and Exponential distributions are the most adequate to account for the concentration of suspended sediments in North America.

However, similar studies related to stream temperatures are scarce. Ouellet et al. (2010) tested eight different distributions at two water temperature stations in the St. Lawrence river (Canada) and found that the Weibull distribution had the best fit for daily maxima. Caissie et al. (2020) successfully fitted a GPD to a 21-year time series of exceedances above a threshold at a single station in Eastern Canada. Much work is still required to understand river temperature regimes and to identify the most adequate distributions to model this variable in various regions of the world.

Different goodness of fit criteria are used to evaluate the adequacy of probability distribution functions (pdf). The most used criteria is presented in this paper are the Akaike (AIC) (Akaike, 1974) and the Bayesian information criteria (BIC) (Schwarz, 1978).

An alternative method for the evaluation of the goodness-of-fit of statistical distributions to sets of observations are the Moment Ratio Diagrams and their variant L-Moment Ratio Diagrams (MRD) (Hosking, 1990). They are commonly applied in hydro-meteorological studies (see for instance El Adlouni et al., 2007a; Ouarda and Charron, 2019) but were never used in river temperature modelling. This approach has the advantage of presenting the skewness and kurtosis of the station data and allowing for an easy comparison of the fit of several pdf on a single

graph. It also allows to analyze the fit of data from several stations on the same graph and to visually identify homogeneous regions. In the present study, LFA and MRD are used to identify the distributions that best fit river temperature data in Switzerland.

This paper is organized as follows: Section 2 presents the methodology used to select the best distribution and to estimate quantiles. Section 3 presents the study area and data used for the analysis. Section 4 provides the results and discussions, with a selection of the most adequate statistical distributions. Finally, conclusions and future works are given in Section 5.

2. Methodology

2.1. Local frequency analysis

LFA is a statistical prediction approach commonly used in hydrology to obtain estimates of the quantiles of extreme events. Based on probabilistic calculations, events' history is used to predict frequencies of future occurrences (e.g. low flow, floods). In this study, LFA is applied to the maximum annual river water temperature in Switzerland.

The main steps in the implementation of this procedure are:

(i) The selection of a sample while respecting the basic statistical hypotheses (homogeneity, stationarity, and independence) and detection of outliers.
(ii) Fitting the model to the data using the most appropriate estimation method.
(iii) Selecting the best distribution to present the data, taking into account the selection criteria.
(iv) Calculation of quantiles (x_T) corresponding to different return periods T; such that the event x_T of return period T corresponds to the quantile of probability of exceedance

$$
\begin{aligned}
&\text{p} = 1/\text{T} = Pr(\text{X} \geq \text{x}_\text{T}). \\
&\text{Thus } Pr(\text{X} \leq \text{x}_\text{T}) = \text{F}\left(\text{x}_\text{T}; \theta_-\right) = 1 - 1/\text{T}, \\
&\text{and } x_T = F^{-1}\left(1 - 1\Big/T; \theta_-\right)
\end{aligned}
\tag{1}
$$

Where F^{-1} corresponds to the inverse cumulative distribution function, θ_- is the vector of parameters, and x_T is the quantile corresponding to return period T or probability of exceedance $p = 1/T$.

2.1.1. Hypotheses testing

It is essential to verify that the data collected respect the conditions of stationarity (Kendall's test described in Mann (1945)), independence (Wald-Wolfowitz's test described in Wald and Wolfowitz (1943)), and homogeneity (Wilcoxon's test described in Wilcoxon (1946)).

2.1.2. Fitting of distributions and estimation methods

To fit a probability distribution, the sample data are sorted in order, and each event is assigned an empirical probability (*Pi*) of exceedance. The Cunnane formula (Cunnane, 1978) is used in the present study:

$$
Pi = \frac{i - \alpha}{N + 1 - 2\alpha}
\tag{2}
$$

Where N represents the sample size to be studied, i is the rank of the observation, and α is a coefficient whose value ranges between 0 and 0.5.

A number of statistical distributions have been used for modeling different hydro-climatological extremes. Table 1 presents the most commonly used distributions in hydrology (El Adlouni et al., 2008; Farooq et al., 2018); and which are generally divided into three groups: the Pearson Type 3 (P3) family (Log-Pearson Type 3 (LP3), Gamma (G), Pearson Type 3 (P3)), the Normal (N) family (Log-Normal (LN), Normal (N)), and the General Extreme-Values (GEV) family (Weibull (W), Gumbel (EV1), Fréchet (EV2)).

To fit statistical models to the data, different parameter estimation methods are available, such as the maximum likelihood (ML) method (El Adlouni et al., 2007b; Smith, 1985), and the method of moments (MM) and its variants (Ashkar and Ouarda, 1996).

2.1.3. Goodness of fit criteria

A number of goodness of fit criteria can be used to compare and select the best fitting distribution. The most commonly used ones are the Akaike Information Criterion (AIC) (Akaike, 1974) and the Bayesian Information Criterion (BIC) (Schwarz, 1978). Both criteria are based on the likelihood function and enable the comparison of the adequacy of a number of distributions for given data set. These criteria are defined as follows:

$$
AIC = -2log(L) + 2k
\tag{3}
$$

$$
BIC = -2log(L) + 2klog(N)
\tag{4}
$$

Where L is the likelihood function, k is the number of parameters, and N is the sample size.

AIC and BIC criteria have the advantage of taking into account the principle of parsimony, i.e. the selection of the most adequate model with a minimum number of parameters. The best fit corresponds to the lowest value of the AIC and BIC (Rao and Hamed, 2019). In the present study, these two criteria are used for the identification of the most adequate distributions for the maximum water temperature in Swiss rivers.

2.2. Theoretical background on L-Moment ratio diagrams

L-moments are linear combinations of probability weighted moments (PWM) (Hosking, 1990). The advantage of L-moments is that they can select a wider range of distributions. Greenwood et al. (1979) defined PWM as:

$$
\beta_r = E\{X[F(X)]^r\}
\tag{5}
$$

where $F(X)$ is the cumulative distribution function of a random variable X and β_r is the rth-order PWM.

Linear combinations of PWM can be interpreted as measures of location, scale and shape of the probability distribution. The rth L-moment λr is related to the rth PWM are defined by (Hosking, 1990) as follows:

$$
\lambda_{r+1} = \sum_{k=0}^{r} p_{r,k}^* \beta_k,
\tag{6}
$$

Where

$$
p_{r,k}^* = (-1)^{r-k} \binom{r}{k} \binom{r+k}{k}
\tag{7}
$$

The dimensionless L-moment ratios, L-variation τ_2 (L-*Cv*), L-skewness τ_3 (L-*Cs*), and L-kurtosis τ_4 (L-*Ck*), are defined as follows:

$$
\tau_2 = \lambda_2/\lambda_1
\tag{8}
$$

$$
\tau_3 = \lambda_3/\lambda_2
$$

$$
\tau_4 = \lambda_4/\lambda_2
$$

An important property of L-moments that makes them attractive for assessing goodness of fit with MRD is that if the mean of the distribution exists, then all L-moments exist and the L-moments uniquely define the distribution (Hosking and Wallis, 2005). In MRD, τ_4 is generally plotted against τ_3. Distribution functions are represented in MRD as a point, a curve or a zone depending on the number of shape parameter of the distribution (Hosking and Wallis, 2005; Ouarda et al., 2016). The pdfs used in the present study are illustrated in Table 1 with their domain and
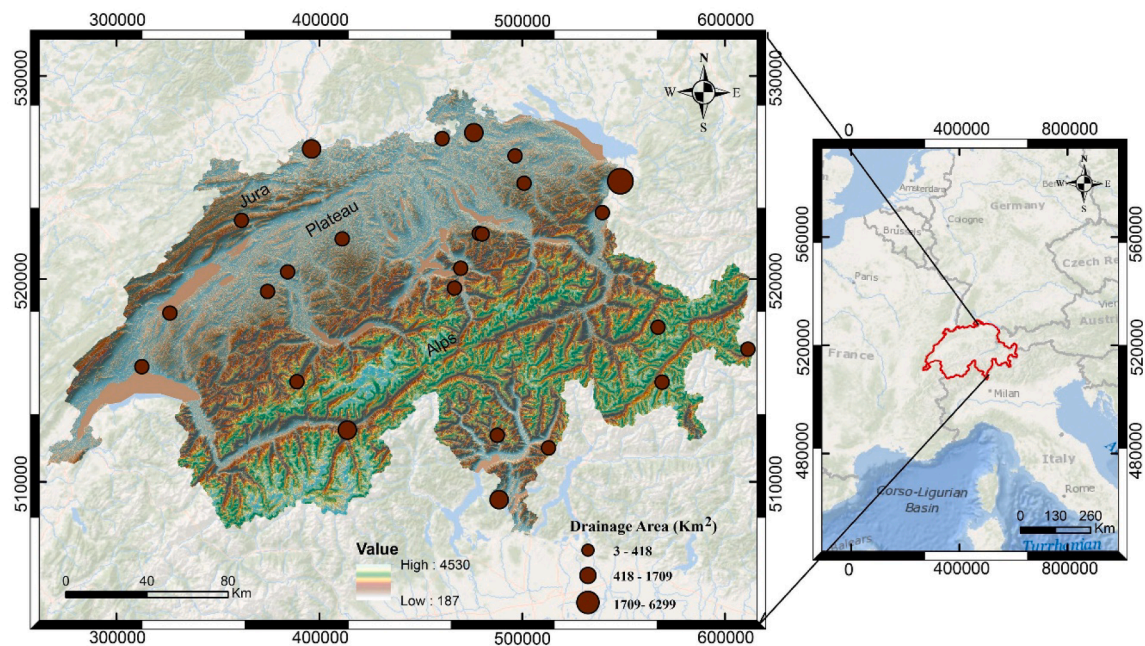
Fig. 1. Spatial distribution of the water temperature stations used in this study.

Table 2
Physiographic characteristics of the 25 selected hydrological catchments in Switzerland.

Basin number	Name	Basin area (km²)	Gauging station altitude (m)	Mean basin altitude (m)	Glacier Cover (%)	Temperature measurement period
1	Birs in Münchenstein	942.92	271.23	753.26	0	1972–2019
2	Murg in Wängi	85.03	473.78	644.18	0	2002–2019
3	Tresa in PonteTresa	609.14	330.13	755.66	0	2002–2019
4	Sense in Thorishaus	351.91	556.89	1068.97	0	2004–2019
5	Allenbath in Adelboden	28.82	1346.64	1853.82	0	2002–2019
6	Rosegbach in Pontresina	66.52	1776.69	2698.32	25.16	2004–2019
7	Grosstalbalch in Isenthal	56.3	795.77	1802.52	4.8	2004–2019
8	Suze in Sonceboz	127.08	653.13	1036.65	0	2004–2019
9	Dischmach in Davos	43.67	1697.74	2368.99	1.19	2004–2019
10	Langeten in Huttwil	60.33	610.83	760.82	0	2002–2019
11	Riale di Roggiasca in Roveredo	8.12	1002.23	1697.22	0	2003–2019
12	Vispa in Visp	778.22	656.47	2659.03	26.02	2002–2019
13	Mentue in Yvonand	104	447.07	679.65	0	2002–2019
14	Liechtensteiner Binnenkanal in Ruggel	108.45	435	861.19	0	1991–2019
15	Reitholzbach in Mosnang	2.76	728.98	789.05	0	2002–2019
16	Glott in Rheinsfleden	417.92	360	501.97	0	1976–2019
17	Venoge in Ecublens	207.15	393.56	678.03	0	2002–2019
18	Rhein in Diepoldsau	6299.19	410.91	1832.81	0.55	1984–2019
19	Worble in Ittigen	63.68	522.94	683.06	0	1988–2019
20	Biber in Biberbrugg	31.95	831.14	1000.12	0	2002–2019
21	Alp in Einsiedeln	46.47	895.86	1154.99	0	2004–2019
22	Riale di Pincascia in Lavertezzo	44.28	585.70	1703.39	0	2004–2019
23	Rom in Müstair	129.17	1241.31	2186.18	0	2002–2019
24	Thur in Andelfingen	1709.42	361.48	775.61	0	1970–2019
25	Muoto in Ingenbohl	314.76	439.68	1365.54	0	1974–2019

number of parameters. Sample L-moments ratios are then plotted on the MRD diagram for all stations.

L-moments are estimated from a finite sample. Let's define $X_{1:n} \leq X_{2:n} \leq \cdots \leq X_{n:n}$, an ordered sample of size n, an unbiased estimator of the rth probability weighted moment Br can be estimated (b_r) as:

$$b_r = n^{-1} \binom{n-1}{r}^{-1} \sum_{j=r+1}^{n} \binom{j-1}{r} x_{j:n} \tag{9}$$

The L-moments of the sample are estimated by:

$$\ell_{r+1} = \sum_{k=0}^{r} p_{r,k}^* b_k, r = 0, 1, ..., n-1. \tag{10}$$

Similar to Eq. (8) The L-moments ratios of the sample are estimated as follows:

$$t_2 = \ell_2 / \ell_1 \tag{11}$$
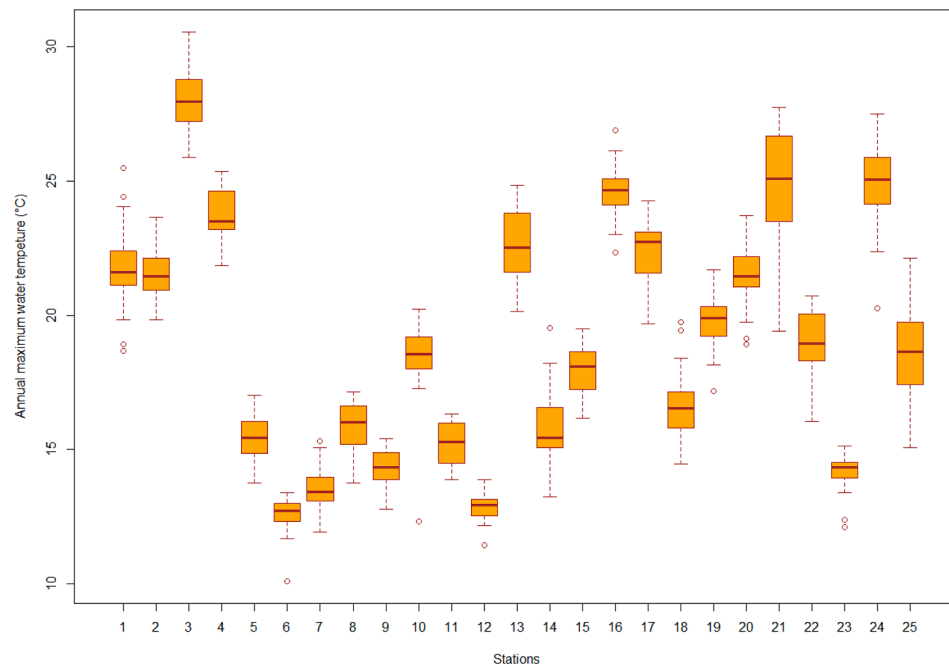
$$t_3 = \ell_3 / \ell_2$$

$$t_4 = \ell_4 / \ell_2$$

Fig. 2. Box plots of the maximum annual water temperatures (°C).

Table 3
Characteristics of the annual maximum river temperature series.

Basin number	Name	Maximum (°C)	Minimum (°C)	Median (°C)	Mean (°C)	SD (°C)	C_V	C_S	C_K
1	Birs in Münchenstein	25.48	18.67	21.59	21.74	1.29	0.05	0.29	0.74
2	Murg in Wängi	23.65	19.84	21.45	21.49	1	0.04	0.32	−0.48
3	Tresa in PonteTresa	30.54	25.88	27.94	28	1.19	0.04	0.13	−0.62
4	Sense in Thorishaus	25.37	21.84	23.5	23.65	1.06	0.04	−0.15	−1.16
5	Allenbath in Adelboden	17.04	13.77	15.43	15.43	0.89	0.05	−0.05	−0.67
6	Rosegbach in Pontresina	13.4	10.11	12.72	12.54	0.78	0.06	−1.76	3.07
7	Grosstalbalch in Isenthal	15.31	11.92	13.42	12.54	0.84	0.06	0.41	−0.14
8	Suze in Sonceboz	17.15	13.77	16.01	12.54	0.98	0.06	−0.55	−0.85
9	Dischmach in Davos	15.4	12.78	14.35	12.54	0.74	0.05	−0.32	−0.8
10	Langeten in Huttwil	20.24	12.33	18.56	12.54	1.67	0.09	−2.35	6.08
11	Riale di Roggiasca in Roveredo	16.32	13.89	15.28	12.54	0.78	0.05	−0.12	−1.56
12	Vispa in Visp	13.9	11.46	12.94	12.54	0.56	0.04	−0.53	0.21
13	Mentue in Yvonand	24.83	20.14	22.51	12.54	1.38	0.06	0.03	−1.08
14	Liechtensteiner Binnenkanal in Ruggel	19.53	13.25	15.45	12.54	1.37	0.08	0.69	0.07
15	Reitholzbach in Mosnang	19.49	16.18	18.09	12.54	0.93	0.05	−0.36	−0.87
16	Glott in Rheinsfleden	26.88	22.33	24.66	12.54	0.87	0.03	−0.17	0.29
17	Venoge in Ecublens	24.26	19.69	22.73	12.54	1.33	0.05	−0.39	−0.97
18	Rhein in Diepoldsau	19.74	14.46	16.53	12.54	1.2	0.07	0.53	0.26
19	Worble in Ittigen	21.68	17.17	19.9	12.54	0.93	0.04	−0.3	0.29
20	Biber in Biberbrugg	23.72	18.93	21.45	12.54	1.35	0.06	−0.23	−0.73
21	Alp in Einsiedeln	27.73	19.4	25.07	12.54	2.35	0.09	−0.69	−0.51
22	Riale di Pincascia in Lavertezzo	20.72	16.06	18.95	12.54	1.2	0.06	−0.62	−0.04
23	Rom in Müstair	15.13	12.13	14.33	12.54	0.81	0.05	−1.2	0.55
24	Thur in Andelfingen	27.49	20.26	25.08	12.54	1.34	0.05	−0.67	1.48
25	Muoto in Ingenbohl	22.12	15.09	18.64	12.54	1.74	0.09	0.003	−0.53

The sample L-moments can be used to select the distribution that best fits the station data, and to choose discordant and homogeneous regions.

2.3. Discordancy test

The discordance Di is measured as a function of L-moments and can be used to determine whether a station should be removed from a given region. Let $u_i = [\tau_{2i} \tau_{3i} \tau_{4i}]^T$ be a vector containing the ratios of L-moments (L-Cv, L-Cs, and L-Ck) for a site i, with the superscript T denoting the transposition of a vector or matrix. The group averages $\bar{u}$ and sample covariance matrix S are presented as follows:

$$\bar{u} = \frac{1}{N} \sum_{i=1}^{N} u_i \tag{12}$$

$$S = \frac{1}{N-1} \sum_{i=1}^{N} (u_i - \bar{u})(u_i - \bar{u})^T \tag{13}$$

And

$$D_i = \frac{1}{3} (u_i - \bar{u})^T S^{-1} (u_i - \bar{u}) \tag{14}$$

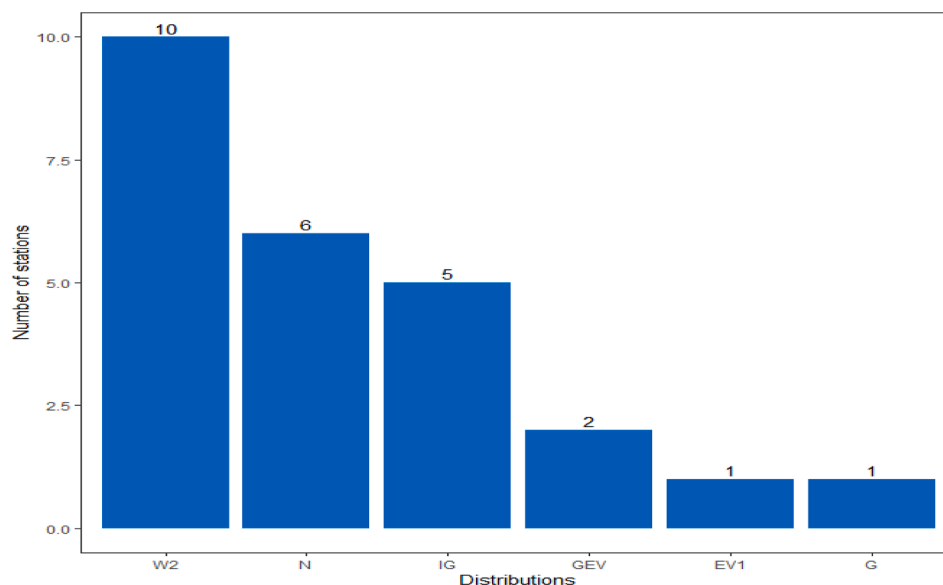Where N is the total number of sites. Note that the average of Di across
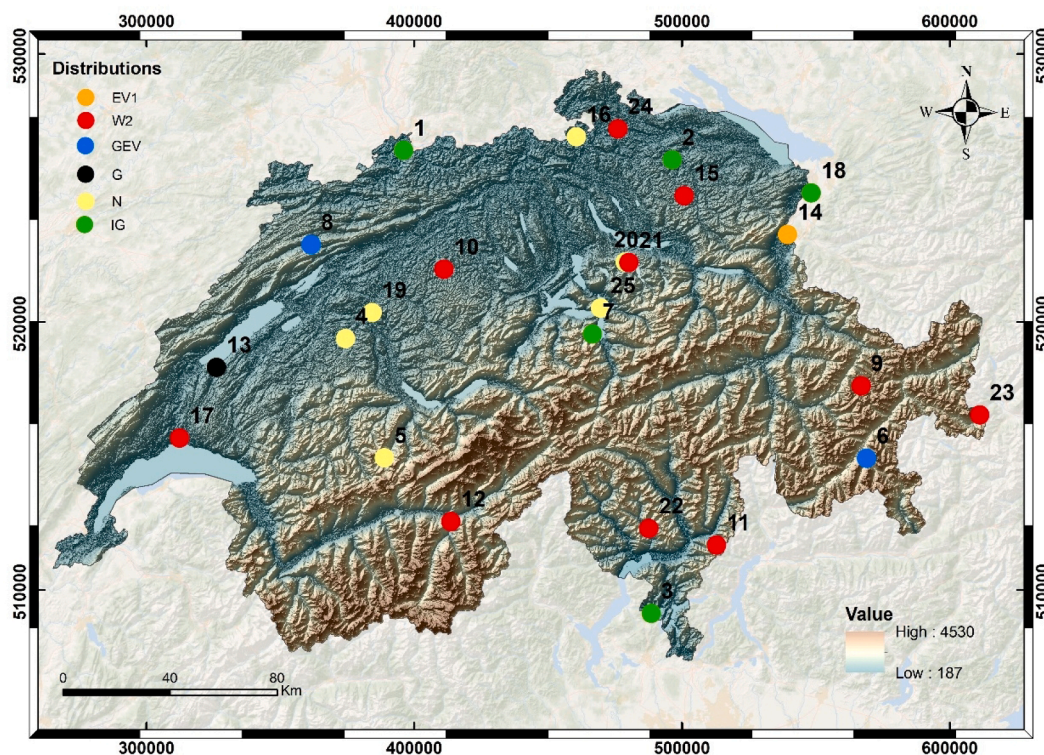
Fig. 3. Distributions selected by AIC criteria.

Fig. 4. Geographic distribution of best fitted pdfs to the maximum annual stream temperatures.

all sites is 1. If Di exceeds 3 for a site, its data are considered to be inconsistent with the rest of the regional data and two possibilities should be investigated; Either there may be an error in the data or the station may actually belong to another region, or no region at all.

3. Study area and data description

Daily water temperature data were provided by the Swiss Federal Office for the Environment (FOEN). Water temperature has only been recorded since the 1960s. Thus, stream temperature time series are relatively short in most stations, varying between 15 and 49 years. The original raw data include 45 watersheds characterised by a wide range of drainage areas (from a few square kilometers to tens of thousands of square kilometers) as well as a wide range of elevations (between 678 m and 2950 m). Switzerland is characterized by a very complex topography which results in fast changes from liquid to solid precipitation even on small spatial scales. The study area can be subdivided into two main zones with different hydrological regimes (Aschwanden and Weingartner, 1985; Michel et al., 2020):

The plateau region and Jura: these areas are marked by low altitudes and a relatively mild climate. Precipitation falls in liquid form during winter and the daily air temperature does not exceed 30 °C during

Table 4
Ranking of D/Ms for all stations based on the goodness-of-fit criteria.

Criteria	Number	Name	Rank of D/M					
			1st	2nd	3rd	4th	5th	6th
AIC	1	Birs in Münchenstein	IG/ML	LN2/ML	G/ML	G/MM	N/ML	LN3/ML
	2	Murg in Wängi	IG/ML	LN2/ML	G/ML	G/MM	N/ML	EV1/WMM
	3	Tresa in PonteTresa	IG/ML	LN2/ML	G/ML	G/MM	N/ML	EV1/ML
	4	Sense in Thorishaus	N/ML	G/ML	G/MM	LN2/ML	IG/ML	LN3/MM
	5	Allenbath in Adelboden	N/ML	G/ML	G/MM	LN2/ML	IG/ML	W2/ML
	6	Rosegbach in Pontresina	GEV/ML	W2/ML	W2/MM	N/ML	G/ML	G/MM
	7	Grosstalbalch in Isenthal	IG/ML	LN2/ML	G/ML	G/MM	N/ML	EV1/ML
	8	Suze in Sonceboz	GEV/ML	W2/ML	W2/MM	GEV/WMM	GEV/MM	N/ML
	9	Dischmach in Davos	W2/ML	W2/MM	N/ML	G/M	GEV/ML	G/MM
	10	Langeten in Huttwil	W2/ML	GEV/ML	W2/MM	N/ML	G/ML	G/MM
	11	Riale di Roggiasca in Roveredo	W2/ML	W2/MM	N/ML	G/ML	G/MM	LN2/ML
	12	Vispa in Visp	W2/ML	W2/MM	N/ML	G/ML	G/MM	LN2/ML
	13	Mentue in Yvonand	G/ML	G/MM	LN3/MM	N/ML	LN2/ML	IG/ML
	14	Liechtensteiner Binnenkanal in Ruggel	EV1/ML	EV1/WMM	EV1/MM	IG/ML	LN2/ML	G/ML
	15	Reitholzbach in Mosnang	W2/ML	W2/MM	N/ML	G/ML	G/MM	LN2/ML
	16	Glott in Rheinsfleden	N/ML	G/ML	G/MM	LN2/ML	IG/ML	GG/ML
	17	Venoge in Ecublens	W2/ML	W2/MM	GEV/ML	N/ML	GEV/WMM	G/ML
	18	Rhein in Diepoldsau	IG/ML	LN2/ML	G/ML	G/MM	EV1/ML	EV1/WMM
	19	Worble in Ittigen	N/ML	G/ML	G/MM	LN2/ML	IG/ML	W2/ML
	20	Biber in Biberbrugg	N/ML	W2/ML	G/ML	G/MM	W2/MM	LN2/ML
	21	Alp in Einsiedeln	W2/ML	W2/MM	GEV/ML	GEV/WMM	P3/ML	GEV/MM
	22	Riale di Pincascia in Lavertezzo	W2/ML	W2/MM	GEV/ML	GEV/MM	P3/ML	N/ML
	23	Rom in Müstair	W2/ML	P3/ML	GEV/ML	GG/MM	P3/ML	LP3/GMM
	24	Thur in Andelfingen	W2/ML	W2/MM	GG/ML	P3/ML	GEV/ML	P3/MM
	25	Muoto in Ingenbohl	N/ML	G/ML	G/MM	LN2/ML	IG/ML	GEV/ML
BIC	1	Birs in Münchenstein	IG/ML	LN2/ML	G/ML	G/MM	N/ML	LN3/ML
	2	Murg in Wängi	IG/ML	LN2/ML	G/ML	G/MM	N/ML	EV1/WMM
	3	Tresa in PonteTresa	IG/ML	G/ML	LN2/ML	G/MM	N/ML	EV1/ML
	4	Sense in Thorishaus	N/ML	G/ML	G/MM	LN2/ML	IG/ML	LN3/MM
	5	Allenbath in Adelboden	N/ML	G/ML	G/MM	LN2/ML	IG/ML	W2/ML
	6	Rosegbach in Pontresina	GEV/ML	W2/ML	W2/MM	N/ML	G/ML	G/MM
	7	Grosstalbalch in Isenthal	IG/ML	LN2/ML	G/ML	G/MM	N/ML	EV1/ML
	8	Suze in Sonceboz	**W2/ML**	**W2/MM**	**GEV/ML**	**N/ML**	**GEV/WMM**	**G/ML**
	9	Dischmach in Davos	W2/ML	W2/MM	N/ML	**G/M**	**G/MM**	**LN2/ML**
	10	Langeten in Huttwil	W2/ML	GEV/ML	W2/MM	N/ML	G/ML	G/MM
	11	Riale di Roggiasca in Roveredo	W2/ML	W2/MM	N/ML	G/ML	G/MM	LN2/ML
	12	Vispa in Visp	W2/ML	W2/MM	N/ML	G/ML	G/MM	LN2/ML
	13	Mentue in Yvonand	G/ML	G/MM	LN3/MM	N/ML	LN2/ML	IG/ML
	14	Liechtensteiner Binnenkanal in Ruggel	EV1/ML	EV1/WMM	EV1/MM	IG/ML	LN2/ML	G/ML
	15	Reitholzbach in Mosnang	W2/ML	W2/MM	N/ML	G/ML	G/MM	LN2/ML
	16	Glott in Rheinsfleden	N/ML	G/ML	G/MM	LN2/ML	IG/ML	GG/ML
	17	Venoge in Ecublens	W2/ML	W2/MM	GEV/ML	N/ML	**G/ML**	**G/MM**
	18	Rhein in Diepoldsau	IG/ML	LN2/ML	G/ML	G/MM	EV1/ML	EV1/WMM
	19	Worble in Ittigen	N/ML	G/ML	G/MM	LN2/ML	IG/ML	W2/ML
	20	Biber in Biberbrugg	N/ML	W2/ML	G/ML	G/MM	W2/MM	LN2/ML
	21	Alp in Einsiedeln	W2/ML	W2/MM	GEV/ML	GEV/WMM	P3/ML	GEV/MM
	22	Riale di Pincascia in Lavertezzo	W2/ML	W2/MM	GEV/ML	**N/ML**	P3/ML	**GEV/MM**
	23	Rom in Müstair	W2/ML	**W2/MM**	**P3/ML**	**GEV/ML**	**GG/MM**	**P3/MM**
	24	Thur in Andelfingen	W2/ML	W2/MM	**N/ML**	**GG/ML**	**P3/ML**	**GEV/ML**
	25	Muoto in Ingenbohl	N/ML	G/ML	G/MM	LN2/ML	IG/ML	GEV/ML

summer.

The Alpine region: typically subdivided into two parts, southern and northern Alps. The Southern Alps are characterized by medium to high altitudes and a climate influenced by the Mediterranean Sea. This results in warm winters and more precipitation in autumn. In contrast, the Northern Alps are characterized by very high average altitudes with thermal and discharge regimes that are strongly influenced by snowmelt. In these basins, maximum flow occur between March and July, depending on the average altitude and the percentage of ice cover, and minimum flow during winter.

The annual maximum values of water temperature were extracted from daily maximum water temperature series during the summer period (May 1 to October 31). These data were tested for stationarity (Mann-Kendall test), independence (Wald-Wolfowitz test), and homogeneity (Wilcoxon test). All 25 stations that passed the Mann-Kendall test also passed the tests of Wald-Wolfowitz and Wilcoxon and were retained for the remainder of the study. These stations are considered independent and identically distributed and can be used in the

subsequent frequency analysis. The table in Appendix A illustrates the results of the Mann Kendall, Wilcoxon and Wald-Wolfowitz tests for the 25 stations retained for the analysis. The locations of these watersheds are illustrated in Fig. 1 and their physiographic properties are summarized in Table 2. The selected watersheds have spatial coverage over the entire study area.

4. Results and discussions

4.1. Descriptive statistics of data series at IID stations

Annual water temperature maxima for the 25 selected rivers exhibit an important variation from one year to the next and a distinct spatial variation between the stations. Fig. 2 shows box plots of water temperature and the regional variation can be seen between stations.

Table 3 presents descriptive statistics of each station, including the maximum, minimum, median, mean, standard deviation, coefficient of variation (C_V), the coefficient of skewness (C_S), and the coefficient of

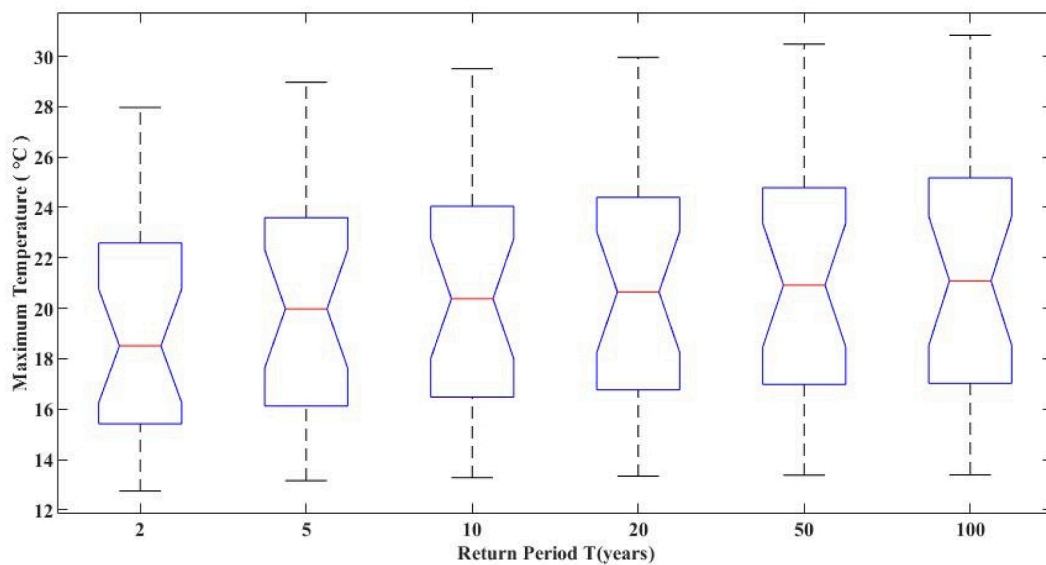**Fig. 5.** Box plots of maximum temperature corresponding to different return periods.
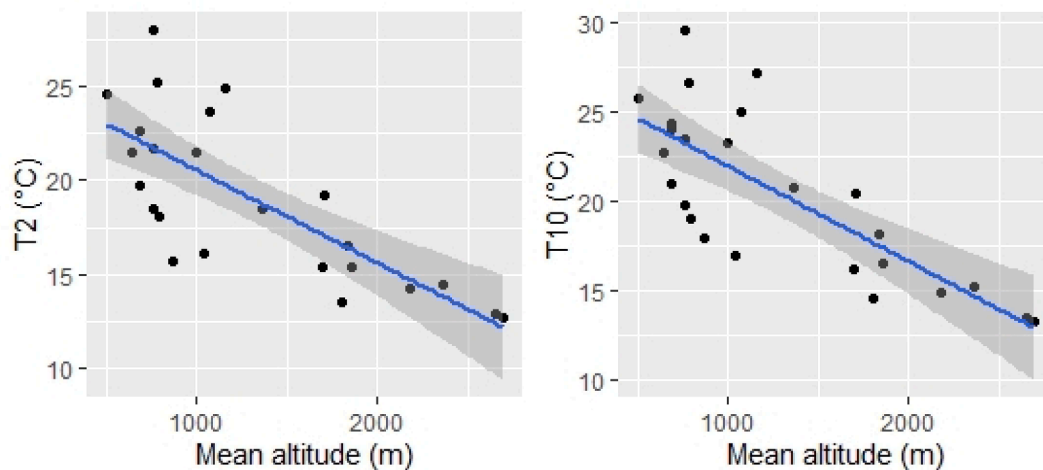

Fig. 6. Relation between quantiles and the average altitude of watersheds.

kurtosis (C_K). It shows that: The average water temperature varies between 12.54 and 28 °C. The C_V are modestly low. The C_S take positive and negative values, suggesting that some distributions are right-skewed and others left-skewed. The C_K show leptokurtic and platykurtic distributions.

4.2. Frequency analysis

The distributions listed in Section 2 are fitted at each station to the maximum annual water temperature. The two-parameter distributions used in this study are the (W2, N, G, EV1 and IG). These distributions are adopted for 92% of the data series. Fig. 3 illustrates the most adequate probability distributions to model extreme stream temperature series based on the AIC criterion.

The W2 distribution is adopted for 40% of the data series (Fig. 3). The remaining 60% of the maximum water temperature series are better fitted with other probability distributions: 24% of the stations are fitted with the N distribution, 20% with the IG, 8% with the GEV and 4% with the G or EV1 distributions. The results are similar using the BIC criterion except 44% of the stations are selected with the W2 and 4% with the GEV.

Fig. 4 indicates that the W2, N and IG distributions are the most frequently selected in the Study Area. Fig. 4 indicates also that some distributions are more predominant in certain regions, suggesting that it may be possible to identify regional distributions. In high altitude areas, the W2 distribution is dominant and many stations located in low to medium altitudes are fitted with the N distribution. There is however no dominant distribution in other parts of Switzerland, leading to some spatial heterogeneity in the selected distribution. Certain rivers that are close geographically, are fitted with different statistical distributions: for instance, the Biber in Biberbrugg river (20) with the N distribution and the Alp in Einsiedeln (21) with W2.

Table 4 lists the 6 best distributions according to the AIC and BIC selection criteria. For each distribution, the candidate distribution/ method (D/M) leading to the best fit is listed. Based on AIC, W2/ML is the best D/M combination for 10 stations, followed by the N/ML combination which is selected for six stations. IG/ML is selected as the best distribution for five stations. Based on BIC, W2/ML is the best D/M combination for 11 stations. N/ML, is the second best D/M combination for six stations. It is also important to note that the most widely used parameter estimation method for all first choices is ML. The differences in the performance of AIC and BIC are minor and affect only a few

Table 5
Results of the L moment and discordancy test.

Basin number	Name	L-Cv	L-Cs	L-Ck	Di
1	Birs in Münchenstein	0.71	0.04	0.16	0.65
2	Murg in Wängi	0.57	0.04	0.11	0.74
3	Tresa in PonteTresa	0.69	0.02	0.1	0.57
4	Sense in Thorishaus	0.62	−0.02	0.05	0.55
5	Allenbath in Adelboden	0.51	0	0.09	0.14
6	Rosegbach in Pontresina	0.39	−0.14	0.12	1.84
7	Grosstalbalch in Isenthal	0.47	0.06	0.13	1.67
8	Suze in Sonceboz	0.57	−0.1	0.05	0.74
9	Dischmach in Davos	0.43	−0.03	0.05	0.23
10	Langeten in Huttwil	0.76	−0.26	0.32	3.11
11	Riale di Roggiasca in Roveredo	0.46	−0.02	−0.03	2.63
12	Vispa in Visp	0.31	−0.03	0.07	0.52
13	Mentue in Yvonand	0.81	0.01	0.08	0.31
14	Liechtensteiner Binnenkanal in Ruggel	0.76	0.15	0.14	2.26
15	Reitholzbach in Mosnang	0.54	−0.06	0.07	0.21
16	Glott in Rheinsfleden	0.49	−0.03	0.09	0.97
17	Venoge in Ecublens	0.77	−0.1	0.07	0.48
18	Rhein in Diepoldsau	0.67	0.06	0.13	0.74
19	Worble in Ittigen	0.53	−0.02	0.1	0.3
20	Biber in Biberbrugg	0.77	−0.04	0.16	0.07
21	Alp in Einsiedeln	1.34	−0.28	0.23	2.54
22	Riale di Pincascia in Lavertezzo	0.68	−0.08	0.09	0.21
23	Rom in Müstair	0.43	−0.13	0.12	1.36
24	Thur in Andelfingen	0.76	−0.04	0.12	0.06
25	Muoto in Ingenbohl	1	−0.01	0.12	2.09

stations (shown in bold in Table 4). As mentioned earlier, there are regions in which most or all stations are fitted with the same distribution. For instance, W2/ML dominates the high-altitude areas, apart from Station 6, which has GEV/ML as the best combination and W2/ML as its second-best choice. Therefore, we can deduce that high altitude regions

are well fitted with W2/ML. Low and medium altitude regions are generally identified by N/ML (stations 5, 4, 16, 19, 20 and 25). In the other stations in low altitude regions, the N/ML is systematically among the four best options. For instance, the N/ML is the third choice in Station 24 (according to BIC), and in Station 15 (according to AIC and BIC). N/ML seems hence to be the most suitable D/M for low to medium altitude areas.

4.3. Estimation of quantiles

Extreme water temperatures limit the distribution of various species of fish in streams. To estimate the upper limits of thermal tolerance in a probabilistic framework, we use the concept of quantiles during the summer period corresponding to different return periods. The results of the maximum stream temperature quantiles corresponding to the selected return periods of 2, 5, 10, 20, 50, and 100 years are presented in Fig. 5 with boxplots. The results of the model revealed that the rivers had changed their thermal regimes (Fig. 5). This thermal stress is an important factor that explains the decline of brown trout in Switzerland (Burkhardt-Holm et al., 2002). Therefore, as mentioned in Section 1, the high water temperature also favors the emergence of diseases. As an illustration, PKD is associated with a seasonal increase in water temperature above 15 °C in brown trout populations (Chilmonczyk et al., 2002). In conformity with Fig. 5, most stations have extreme temperatures that exceed this threshold even in low return periods. In addition, Elliott (2001) reported that brown trout achieve maximum growth at 13.1–13.9 °C. According to the results of this study, this temperature is found in most Switzerland rivers. The lethal temperature of 29.7 °C is reached at certain stations for the 20-year return period (Elliott, 1981). On the other hand, thermal stress also affects energy storage levels and metabolic rates (Álvarez et al., 2006). Additionally, fecundity decreases with increasing temperature while egg size increases (Jonsson and Jonsson, 2009).

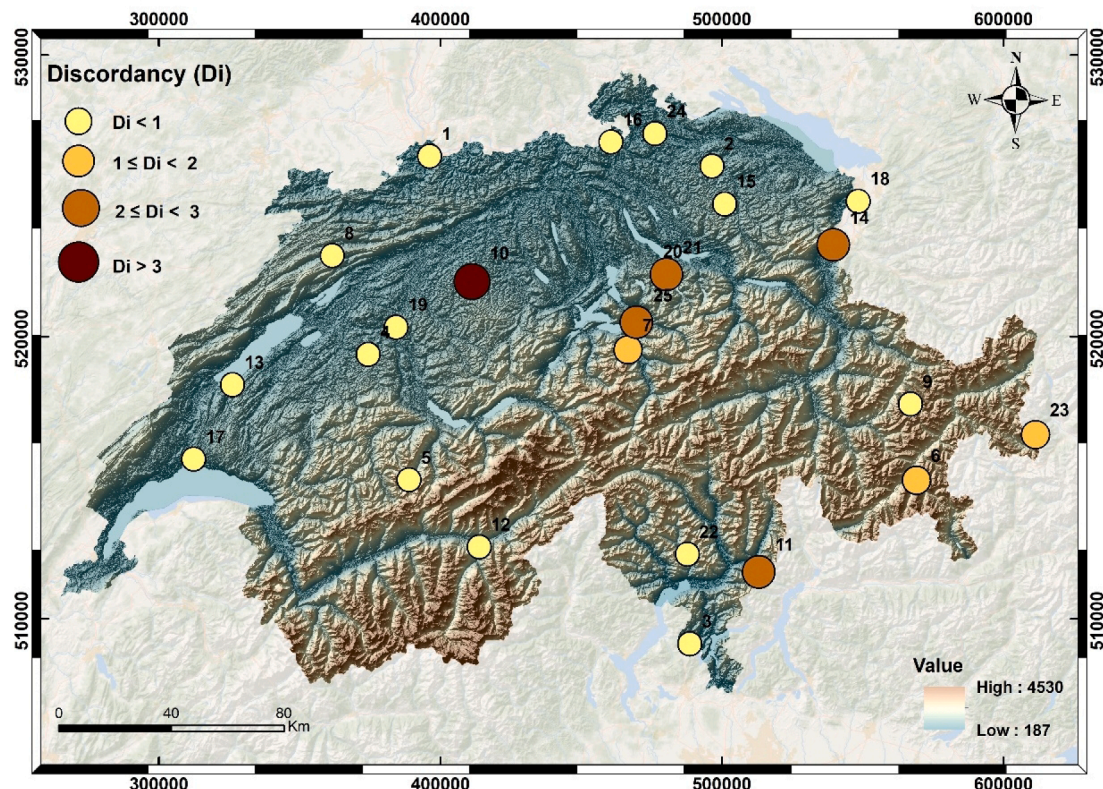In addition, it would be interesting to determine the duration of fish

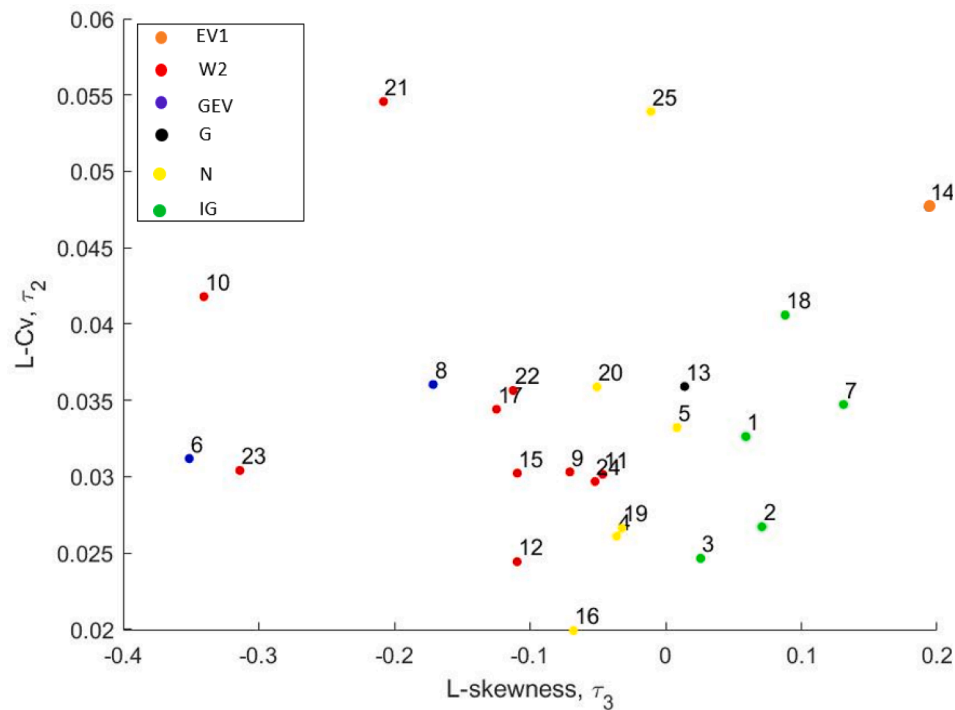**Fig. 7.** Spatial distribution of discordancy test of the maximum water temperature.

Fig. 8. Relationship between L coefficient of variation and L-skewness of maximum annual water temperatures.
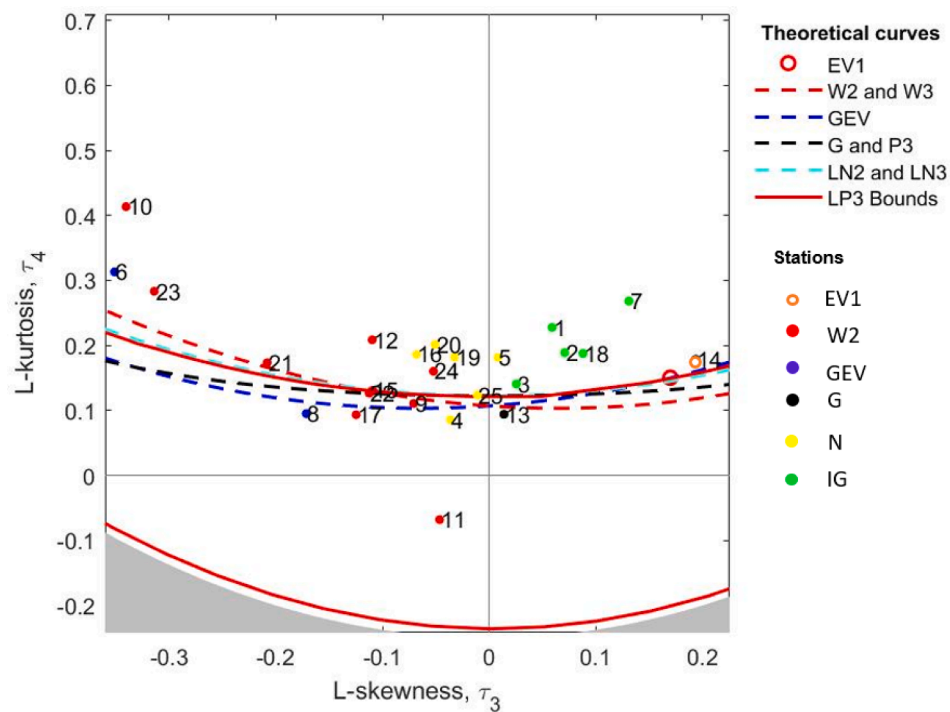

Fig. 9. L moments ratio Diagram of water temperature stations.

exposure to high temperatures. This study showed the merit of using maximum water temperature quantiles as an ecological indicator. Using brown trout thermal requirements as an example, we demonstrated that the quantile and its associated return period could provide insight into the relative thermal risk for this species in Swiss rivers. However, our study did not include the notion of duration of stressful events. This could be done by implementing a Peaks Over Threshold approach, as indicated by Caissie et al. (2020). In this approach, it is possible to model

events for which temperatures exceed a certain threshold instead of focusing on annual or seasonal maxima. The duration of the exceedance can be quantified, and the degree-days cumulated during these exceedance events can be computed. However, this approach is more complex and may be more difficult to implement for water resources managers.

4.4. Correlation of quantiles with the mean watershed altitude

Naturally, Fig. 6 indicates that there is a strong negative correlation between water temperature extremes corresponding to different return periods and the mean altitude of the catchments. The correlation coefficient between the mean altitude and the 2-year return period quantile is equal to −0.763 and with the 10-year return period quantile it is equal to −0.773. Therefore, lower-altitude basins are naturally more likely to have higher extreme values. This may explain the relocation of brown trout habitat to higher altitudes and alpine rivers (Hari et al., 2006).

4.5. Discordancy test

The L-*Cv*, L-*Cs*, L-*Ck*, and the discordance (Di) values for all 25 stations are presented in Table 5. They suggest that the majority of the study area is homogeneous, with Di values below 3. There is only one station (Site 10) where Di is equal to 3.11.

Fig. 7 illustrates the spatial distribution of the discordancy test results and Fig. 8 presents the relationship between L-Cv and L-Cs of maximum annual water temperatures. The Fig. 7 reveals that the low altitude regions (Jura and Plateau) are homogeneous, with Di < 1 for 11 sites. The middle altitude regions are not definitively homogeneous (2 ≤ Di < 3), and they have elevated L-*Cv* (sites 21, 25, 14) in Fig. 8. For high elevation regions, there are homogeneous sites (9, 12, and 22) where Di < 1, and other likely homogeneous sites (1 ≤ Di < 2) for example sites (6 and 23), and that have very low L-*Cv*. According to classical discordant measurements (Di), only station 10 is considered a discordant site. L-*Cv* - L-*Cs* figure also shows a certain regional aspect, as samples with the same distribution in LFA are grouped in the same regions.

4.6. L-moment ratio diagram

The method of the MRD is also used as an alternative method for selecting pdfs and comparing them with the distributions adopted based on selection criteria. Sample L-moments are measured for each water temperature series using Eqs. (10) and (11) and each station is represented in the MRD. The results are shown in Fig. 9 where each station is numbered according to its rank in Table 5. The analysis of this diagram leads to the following conclusions about the suitability of the pdfs to fit the stations sample data. the curve of W2-W3 goes through the middle of the scatter of stations. The majority of stations are located outside the LP3 domain. As illustrated in the Fig. 9 of the MRD, there are stations that are well fitted with W2-W3 (21, 15, 9 and 22), with GEV (8) and with EV1 (14). In addition, this diagram shows a clear regional clustering of stations i.e. there are regions that can be considered as thermally homogeneous. Stations that were fitted with the same distribution in LFA are identified on MRD by the same color. The majority of stations in red are well fitted with W2 also according to MRD and are located in high altitude regions, except for Station 11, which has a Di = 2.63 and is located far from the W2 line on the MRD. Stations in yellow are fitted with the normal distribution and are located in low-altitude regions. According to MRD, station 24 is better fitted with the N distribution, which is the third best choice according to the BIC criterion. Stations in green are fitted with IG and in the MRD they are located close to the LN2-LN3 curve, which is generally the second choice according to AIC and BIC. A high level of concordance is hence observed between the

MRD, the AIC/BIC analysis and the discordancy test.

5. Conclusions and future works

AIC and BIC were used to evaluate the goodness of fit of statistical distributions for maximum river temperature data in Switzerland. In general, the lowest values of AIC and BIC are observed for distributions with two parameters. It was found that W2 fits properly high-altitude stations, while stations in lower altitude regions are well fitted with the N distribution. This points out to a significant level of regional homogeneity in the study area. The frequency analysis indicates high water temperatures for different return periods. These extreme water temperature events were concomitant with fish mortality e.g. brown trout in Switzerland. The median value of quantiles with a 20 year return period exceed 19.5 °C, which is a thermal indicator of stress for juvenile brown trout, as they cease to feed above this temperature. The lower quantiles (e.g. with a return period of two years) could be used as an indicator of risk for PKD proliferation in Brown trout. These indicators could be adapted for the different thermal regions defined herein.

The discordancy analysis of the station data indicates that there is only one site that exceeds the critical value. The MRD method was used to evaluate the adequacy of several pdfs to fit water temperature data. The conclusions based on the MRD are as follows: Visually confirms the existence of homogeneous regions, shows that some stations are located outside the LP3 boundary. The MRD plot also shows a regional pattern, as stations with the same distribution are often located in the same region. This also suggests that the first choice of D/M for some stations may not always be the best one. However, some samples were located far from the distributions curves. In general, MRD results are coherent with the outputs of the AIC and BIC selection criteria.

Future research can focus on the development of regional frequency analysis models for the estimation of water temperature characteristics at ungauged rivers. Future efforts can also aim at the development of nonstationary local and regional frequency analysis models that integrate information concerning climate variability and change.

CRediT authorship contribution statement

Z. Souaissi: Conceptualization, Methodology, Software, Formal analysis, Investigation, Data curation, Visualization, Writing – original draft. **T.B.M.J. Ouarda:** Conceptualization, Methodology, Validation, Investigation, Supervision, Writing – review & editing, Funding acquisition. **A. St-Hilaire:** Conceptualization, Methodology, Validation, Investigation, Supervision, Writing – review & editing.

Declaration of Competing Interest

The authors declare that they have no known competing financial interests or personal relationships that could have appeared to influence the work reported in this paper.

Acknowledgments

Appendix A. Mann Kendall, Wilcoxon and Wald-Wolfowitz test results

Basin number	Name	Mann Kendall		Wilcoxon		Wald-Wolfowitz	
		Statistic	P-value	Statistic	P-value	Statistic	P-value
1	Birs in Münchenstein	1.4666	0.1425	−0.165	0.869	0.1796	0.8575
2	Murg in Wängi	0.7576	0.4487	−1.059	0.2893	0.4747	0.635

(continued on next page)

(*continued*)

Basin number	Name	Mann Kendall		Wilcoxon		Wald-Wolfowitz	
		Statistic	P-value	Statistic	P-value	Statistic	P-value
3	Tresa in PonteTresa	0.3411	0.733	−0.1767	0.8597	0.645	0.5189
4	Sense in Thorishaus	−0.3152	0.7526	0.7877	0.4309	0.5719	0.5674
5	Allenbath in Adelboden	0.8718	0.3833	−0.9277	0.3536	1.3491	0.1773
6	Rosegbach in Pontresina	0.8554	0.3923	−0.8468	0.3971	1.6842	0.0922
7	Grosstalbalch in Isenthal	1.7559	0.0791	−1.2077	0.2271	0.2889	0.7726
8	Suze in Sonceboz	−0.2251	0.8219	0.3676	0.7132	0.4398	0.6601
9	Dischmach in Davos	0.5408	0.5886	−0.7357	0.4619	0.7324	0.4639
10	Langeten in Huttwil	0.5303	0.5959	−0.4415	0.6588	0.0188	0.985
11	Riale di Roggiasca in Roveredo	1.5907	0.1117	−1.2028	0.229	0.6227	0.5335
12	Vispa in Visp	0.9489	0.3426	−1.6361	0.1018	0.0762	0.9392
13	Mentue in Yvonand	1.7424	0.0814	−1.1479	0.251	0.144	0.8855
14	Liechtensteiner Binnenkanal in Ruggel	0.6004	0.5483	−0.7342	0.4628	0.1995	0.8419
15	Reitholzbach in Mosnang	1.1363	0.2558	−1.0596	0.2893	0.1097	0.9127
16	Glott in Rheinsfleden	1.5074	0.1317	−0.6693	0.5033	0.4527	0.6508
17	Venoge in Ecublens	0.0825	0.9343	−0.2407	0.8098	0.642	0.5209
18	Rhein in Diepoldsau	1.4302	0.1527	0.1096	0.9127	0.4266	0.6697
19	Worble in Ittigen	1.0543	0.2917	−0.4192	0.6751	0.959	0.3375
20	Biber in Biberbrugg	0.5686	0.5696	−0.265	0.791	0.4572	0.6476
21	Alp in Einsiedeln	1.3707	0.1705	−1.535	0.1248	0.0543	0.9567
22	Riale di Pincascia in Lavertezzo	0.9455	0.3444	−0.5293	0.5966	0.2247	0.8222
23	Rom in Müstair	1.3193	0.1871	−0.7703	0.4411	1.0637	0.2875
24	Thur in Andelfingen	2.4286	0.0152	−1.7914	0.0732	1.5311	0.1258
25	Muoto in Ingenbohl	2.1968	0.028	−0.6805	0.4962	0.1796	0.8575

References

Akaike, H., 1974. A new look at the statistical model identification. IEEE Trans. Automatic Control 19 (6), 716–723. https://doi.org/10.1109/TAC.1974.1100705.

Álvarez, D., Cano, J.M., Nicieza, A.G., 2006. Microgeographic variation in metabolic rate and energy storage of brown trout: countergradient selection or thermal sensitivity? Evol. Ecol. 20 (4), 345–363.

Aschwanden, H., Weingartner, R., 1985. Die Abflussregimes der Schweiz. https://doi.org/10.7892/boris.133660.

Ashkar, F., Ouarda, T.B.M.J., 1996. On some methods of fitting the generalized Pareto distribution. J. Hydrol. 177 (1-2), 117–141. https://doi.org/10.1016/0022-1694(95)02793-9.

Ashley Steel, E., Sowder, C., Peterson, E.E., 2016. Spatial and temporal variation of water temperature regimes on the snoqualmie river network JAWRA. J. Am. Water Resour. Assoc. 52 (3), 769–787. https://doi.org/10.1111/jawr.2016.52.issue-310.1111/1752-1688.12423.

Beaupré, J., Boudreault, J., Bergeron, N., St-Hilaire, A., 2020. Inclusion of water temperature in a fuzzy logic Atlantic salmon (Salmo salar) parr habitat model. J. Therm. Biol. 87 https://doi.org/10.1016/j.jtherbio.2019.102471.

Benyahya, L., Caissie, D., St-Hilaire, A., Ouarda, T.B.M.J., Bobée, B., 2007. A review of statistical water temperature models. Canad. Water Resour. J. 32 (3), 179–192. https://doi.org/10.4296/cwrj3203179.

Boudreault, J., Bergeron, N.E., St-Hilaire, A., Chebana, F., 2019. Stream Temperature Modeling Using Functional Regression Models JAWRA. J. Am. Water Resour. Assoc. 55 (6), 1382–1400. https://doi.org/10.1111/jawr.v55.610.1111/1752-1688.12778.

Brandão, M.L., Colognesi, G., Bolognesi, M.C., Costa-Ferreira, R.S., Carvalho, T.B., Gonçalves-de-Freitas, E., 2018. Water temperature affects aggressive interactions in a Neotropical cichlid fish. Neotropical Ichthyol. 16 https://doi.org/10.1590/1982-0224-20170081.

Burkhardt-Holm, P., Peter, A., Segner, H., 2002. Decline of fish catch in Switzerland. Aquat. Sci. 64, 36–54.

Caissie, D., 2006. The thermal regime of rivers: a review. Freshw. Biol. 51 (8), 1389–1406. https://doi.org/10.1111/fwb.2006.51.issue-810.1111/j.1365-2427.2006.01597.x.

Caissie, D., Ashkar, F., El-Jabi, N., 2020. Analysis of air/river maximum daily temperature characteristics using the peaks over threshold approach. Ecohydrology 13 (1). https://doi.org/10.1002/eco.v13.110.1002/eco.2176.

Chilmonczyk, S., Monge, D., De Kinkelin, P., 2002. Proliferative kidney disease: cellular aspects of the rainbow trout, Oncorhynchus mykiss (Walbaum), response to parasitic infection. J. Fish Dis. 25, 217–226. https://doi.org/10.1046/j.1365-2761.2002.00362.x.

Cunnane, C., 1978. Unbiased plotting positions—a review. J. Hydrol. 37, 205–222. https://doi.org/10.1016/0022-1694(78)90017-3.

Moore, R.D., Spittlehouse, D.L., Story, A., 2005. Riparian microclimate and stream temperature response to forest harvesting: a review1. JAWRA J. Am. Water Resour. Assoc. 41 (4), 813–834. https://doi.org/10.1111/jawr.2005.41.issue-410.1111/j.1752-1688.2005.tb03772.x.

Dugdale, S.J., Bergeron, N.E., St-Hilaire, A., 2013. Temporal variability of thermal refuges and water temperature patterns in an Atlantic salmon river. Remote Sens. Environ. 136, 358–373. https://doi.org/10.1016/j.rse.2013.05.018.

Dugdale, S.J., Hannah, D.M., Malcolm, I.A., 2017. River temperature modelling: A review of process-based approaches and future directions. Earth Sci. Rev. 175, 97–113. https://doi.org/10.1016/j.earscirev.2017.10.009.

El Adlouni, S., Bobée, B., Ouarda, T.B.M.J., 2008. On the tails of extreme event distributions in hydrology. J. Hydrol. 355 (1-4), 16–33. https://doi.org/10.1016/j.jhydrol.2008.02.011.

El Adlouni, S., Ouarda, T., Bobée, B., 2007a. Orthogonal projection L-moment estimators for three-parameter distributions. Adv. Applications Stat. 7, 193–209.

El Adlouni, S., Ouarda, T.B.M.J., Zhang, X., Roy, R., Bobée, B., 2007b. Generalized maximum likelihood estimators for the nonstationary generalized extreme value model. Water Resour. Res. 43 https://doi.org/10.1029/2005WR004545.

Elliott, H., 2001. Modelling growth of brown trout, Salmo trutta, in terms of weight and energy units. Freshw. Biol. 46, 679–692. https://doi.org/10.1046/j.1365-2427.2001.00705.x.

Elliott, J., 1981. Some aspects of thermal stress on fresh-water teleosts. Stress Fish 209–245.

Elliott, J.M., Elliott, J.A., 2010. Temperature requirements of Atlantic salmon Salmo salar, brown trout Salmo trutta and Arctic charr Salvelinus alpinus: predicting the effects of climate change. J. Fish Biol. 77, 1793–1817. https://doi.org/10.1111/j.1095-8649.2010.02762.x.

Farooq, M., Shafique, M., Khattak, M.S., 2018. Flood frequency analysis of river swat using Log Pearson type 3, Generalized Extreme Value, Normal, and Gumbel Max distribution methods. Arab. J. Geosci. 11, 1–10. https://doi.org/10.1007/s12517-018-3553-z.

Ficklin, D.L., Stewart, I.T., Maurer, E.P., 2013. Effects of climate change on stream temperature, dissolved oxygen, and sediment concentration in the Sierra Nevada in California. Water Resour. Res. 49, 2765–2782. https://doi.org/10.1002/wrcr.20248.

Gallice, A., Schaefli, B., Lehning, M., Parlange, M., Huwald, H., 2015. Stream temperature prediction in ungauged basins: review of recent approaches and description of a new physics-derived statistical model. Hydrol. Earth Syst. Sci. 19, 3727–3753. https://doi.org/10.5194/hess-19-3727-2015.

Greenwood, J.A., Landwehr, J.M., Matalas, N.C., Wallis, J.R., 1979. Probability weighted moments: Definition and relation to parameters of several distributions expressable in inverse form. Water Resour. Res. 15 (5), 1049–1054. https://doi.org/10.1029/WR015i005p01049.

Hari, R.E., Livingstone, D.M., Siber, R., Burkhardt-Holm, P., Güttinger, H., 2006. Consequences of climatic change for water temperature and brown trout populations in Alpine rivers and streams. Glob. Change Biol. 12, 10–26. https://doi.org/10.1111/j.1365-2486.2005.001051.x.

Hosking, J.R.M., 1990. L-moments: Analysis and estimation of distributions using linear combinations of order statistics. J. Royal Stat. Soc. Ser. B (Methodol.) 52 (1), 105–124. https://doi.org/10.1111/rssb:1990.52.issue-110.1111/j.2517-6161.1990.tb01775.x.

Hosking, J.R.M., Wallis, J.R., 2005. Regional frequency analysis: an approach based on L-moments. Cambridge University Press.

Hosseini, N., Johnston, J., Lindenschmidt, K.-E., 2017. Impacts of climate change on the water quality of a regulated prairie river. Water 9, 199. https://doi.org/10.3390/w9030199.

Isaak, D., Wollrab, S., Horan, D., Chandler, G., 2012. Climate change effects on stream and river temperatures across the northwest US from 1980–2009 and implications

for salmonid fishes. Clim. Change 113, 499–524. https://doi.org/10.1007/s10584-011-0326-z.

Isaak, D.J., Rieman, B.E., 2013. Stream isotherm shifts from climate change and implications for distributions of ectothermic organisms. Glob. Change Biol. 19 (3), 742–751. https://doi.org/10.1111/gcb.2013.19.issue-310.1111/gcb.12073.

Jonsson, B., Jonsson, N., 2009. A review of the likely effects of climate change on anadromous Atlantic salmon Salmo salar and brown trout Salmo trutta, with particular reference to water temperature and flow. J. Fish Biol. 75, 2381–2447. https://doi.org/10.1111/j.1095-8649.2009.02380.x.

Körner, O., Kohno, S., Schönenberger, R., Suter, M.J.-F., Knauer, K., Guillette Jr, L.J., Burkhardt-Holm, P., 2008. Water temperature and concomitant waterborne ethinylestradiol exposure affects the vitellogenin expression in juvenile brown trout (Salmo trutta). Aquat. Toxicol. 90, 188–196. https://doi.org/10.1016/j.aquatox.2008.08.012.

Kwak, J., St-Hilaire, A., Chebana, F., Kim, G., 2017. Summer season water temperature modeling under the climate change: case study for Fourchue River, Quebec. Canada Water 9, 346. https://doi.org/10.3390/w9050346.

Maheu, A., St-Hilaire, A., Caissie, D., El-Jabi, N., Bourque, G., Boisclair, D., 2016. A regional analysis of the impact of dams on water temperature in medium-size rivers in eastern Canada. Can. J. Fish. Aquat. Sci. 73 (12), 1885–1897. https://doi.org/10.1139/cjfas-2015-0486.

Mann, H.B., 1945. Nonparametric tests against trend. Econometrica: J. Econometr. Soc. 245–259. https://doi.org/10.2307/1907187.

Michel, A., Brauchli, T., Lehning, M., Schaefli, B., Huwald, H., 2020. Stream temperature and discharge evolution in Switzerland over the last 50 years: annual and seasonal behaviour. Hydrol. Earth Syst. Sci. 24, 115–142. https://doi.org/10.5194/hess-24-115-2020.

Mujere, N., Moyce, W., 2018. In: Hydrology and Water Resource Management: Breakthroughs in Research and Practice. IGI Global, pp. 97–115. https://doi.org/10.4018/978-1-5225-3427-3.ch004.

Niedrist, G.H., Psenner, R., Sommaruga, R., 2018. Climate warming increases vertical and seasonal water temperature differences and inter-annual variability in a mountain lake. Clim. Change 151 (3-4), 473–490. https://doi.org/10.1007/s10584-018-2328-6.

Ouarda, T.B., Charron, C., 2019. Changes in the distribution of hydro-climatic extremes in a non-stationary framework. Sci. Rep. 9, 1–8. https://doi.org/10.1038/s41598-019-44603-7.

Ouarda, T.B., Charron, C., Chebana, F., 2016. Review of criteria for the selection of probability distributions for wind speed data and introduction of the moment and L-moment ratio diagram methods, with a case study. Energy Convers. Manage. 124, 247–265. https://doi.org/10.1016/j.enconman.2016.07.012.

Ouellet, V., Mingelbier, M., Saint-Hilaire, A., Morin, J., 2010. Frequency analysis as a tool for assessing adverse conditions during a massive fish kill in the St. Lawrence River, Canada. Water Qual. Res. J. 45, 47–57. https://doi.org/10.2166/wqrj.2010.006.

Ouellet, V., St-Hilaire, A., Dugdale, S.J., Hannah, D.M., Krause, S., Proulx-Ouellet, S., 2020. River temperature research and practice: Recent challenges and emerging opportunities for managing thermal habitat conditions in stream ecosystems. Sci. Total Environ. 139679 https://doi.org/10.1016/j.scitotenv.2020.139679.

Petts, G.E., 2000. In: Assessing the Ecological Integrity of Running Waters. Springer Netherlands, Dordrecht, pp. 15–27. https://doi.org/10.1007/978-94-011-4164-2_2.

Rao, A.R., Hamed, K.H., 2019. Flood frequency analysis. CRC Press. https://doi.org/10.1201/9780429128813.

Schwarz, G., 1978. Estimating the dimension of a model. Ann. Stat. 6, 461–464. https://doi.org/10.1214/aos/1176344136.

Smith, Richard L., 1985. Maximum likelihood estimation in a class of nonregular cases. Biometrika 72 (1), 67–90. https://doi.org/10.1093/biomet/72.1.67.

St-Hilaire, A., Ouarda, T.B.M.J., Bargaoui, Z., Daigle, A., Bilodeau, L., 2012. Daily river water temperature forecast model with a k-nearest neighbour approach. Hydrol. Process. 26 (9), 1302–1310. https://doi.org/10.1002/hyp.v26.910.1002/hyp.8216.

Strepparava, Nicole, Segner, Helmut, Ros, Albert, Hartikainen, Hanna, Schmidt-Posthaus, Heike, Wahli, Thomas, 2018. Temperature-related parasite infection dynamics: the case of proliferative kidney disease of brown trout. Parasitology 145 (3), 281–291. https://doi.org/10.1017/S0031182017001482.

Sun, L., Chen, H., 2014. Effects of water temperature and fish size on growth and bioenergetics of cobia (Rachycentron canadum). Aquaculture 426-427, 172–180. https://doi.org/10.1016/j.aquaculture.2014.02.001.

Thiombiano, A.N., El Adlouni, S., St-Hilaire, A., Ouarda, T.B.M.J., El-Jabi, N., 2017. Nonstationary frequency analysis of extreme daily precipitation amounts in Southeastern Canada using a peaks-over-threshold approach. Theor. Appl. Climatol. 129 (1-2), 413–426. https://doi.org/10.1007/s00704-016-1789-7.

Tramblay, Yves, St-Hilaire, Andre, Ouarda, Taha B.M.J., 2008. Frequency analysis of maximum annual suspended sediment concentrations in North America/Analyse fréquentielle des maximums annuels de concentration en sédiments en suspension en Amérique du Nord. Hydrol. Sci. J. 53 (1), 236–252. https://doi.org/10.1623/hysj.53.1.236.

Wahli, T., Bernet, D., Segner, H., Schmidt-Posthaus, H., 2008. Role of altitude and water temperature as regulating factors for the geographical distribution of Tetracapsuloides bryosalmonae infected fishes in Switzerland. J. Fish Biol. 73, 2184–2197. https://doi.org/10.1111/j.1095-8649.2008.02054.x.

Wald, A., Wolfowitz, J., 1943. An exact test for randomness in the non-parametric case based on serial correlation. Ann. Math. Stat. 14 (4), 378–388. https://doi.org/10.1214/aoms/1177731358.

Wehrly, K.E., Wang, L., Mitro, M., 2007. Field-based estimates of thermal tolerance limits for trout: incorporating exposure time and temperature fluctuation. Trans. Am. Fish. Soc. 136 (2), 365–374. https://doi.org/10.1577/T06-163.1.

Wilcoxon, F., 1946. Individual comparisons of grouped data by ranking methods. J. Econ. Entomol. 39, 269–270. https://doi.org/10.1093/jee/39.2.269.

Zhu, S., Heddam, S., Nyarko, E.K., Hadzima-Nyarko, M., Piccolroaz, S., Wu, S., 2019. Modeling daily water temperature for rivers: comparison between adaptive neuro-fuzzy inference systems and artificial neural networks models. Environ. Sci. Pollut. Res. 26 (1), 402–420. https://doi.org/10.1007/s11356-018-3650-2.